

Application of Air-Coupled Ultrasonic Transducers for Damage Assessment of Composite Panels

L. AMBROZINSKI, B. PIWAKOWSKI, T. STEPINSKI and T. UHL

ABSTRACT

In this paper we demonstrate how Lamb waves, excited and received by air-coupled transducers, can be used for damage assessment of composite structures. The test setup used in our experiments consisted of a pair of air-coupled transducers that operated in pitch-catch mode in the frequency band 100 to 500 kHz. The transducers were used to scan the inspected surface with the aid of a precise mechanical scanner. Incident angle of the transducers could be set to evoke and receive the desired mode of Lamb waves in the inspected panel. Results of scanning of the inspected panel using different Lamb wave modes are presented in the paper. The experimental setup was very versatile and enabled observation of various wave phenomena, e.g. reflection and mode conversion, occurring at the damage interface. The results presented in the paper illustrate the ways how the phenomena observed during the experiments can be used for damage detection.

INTRODUCTION

Composite structures made of carbon fiber reinforced polymers (CRFP) and glass fiber reinforced polymers (GFRP), are widely used in engineering structures requiring high safety standards. However, large number of failure modes may exist in the composites.

Lukasz Ambrozinski, AGH University of Science and Technology, al. Mickiewicza 30, 30-059 Krakow, Poland, ambrozin@agh.edu.pl
Bogdan Piwakowski, Ecole Centrale de Lille, 59650 Villeneuve d'Ascq B.P. 58 cedex, France, bogdan.piwakowski@ec-lille.fr
Tadeusz Stepinski, AGH University of Science and Technology, al. Mickiewicza 30, 30-059 Krakow, Poland, tstepin@agh.edu.pl
Tadeusz Uhl, AGH University of Science and Technology, al. Mickiewicza 30, 30-059 Krakow, Poland, tuhl@agh.edu.pl

Some of them, for instance porosity and foreign object inclusion, may occur during the manufacturing, other, e.g. disbonds and delaminations, occur often during the exploitation of the structure. Therefore, there is a need for both quality control and monitoring of such structures. Ultrasonic Lamb waves (LW), due to their sensitivity to various failure modes of composite panels are a valuable tool for this purpose.

Excitation and reception of ultrasonic waves by the means of contact transducers requires normally a coupling liquid, for instance, water or an acoustic gel, which can be inconvenient and time-consuming. The measurements can also be performed using contactless methods that do not require coupling agent, e.g. lasers or EMATs. However, a main drawback of a laser source is its cost, and EMATs cannot be applied to investigate nonmetallic structures. Therefore an extensive research has been done in the field of transducers using gases as a coupling medium, particularly air, which is a part of the natural environment [1]. The main problem to solve in the area of air-coupled ultrasound is a large impedance mismatch between solids and air, due to which only a small portion of acoustic energy can be passed between the transmitter and investigated object. Therefore, applications of high-voltage excitation [2] and effective matching layers reducing the impedance mismatch [3] have been proposed. The most promising in imaging applications among all those devices two types of air-coupled transducers seem to be the most promising in imaging applications: the capacitive and piezoelectric [4]. These transducers, however, when applied for the characterization of panels using bulk waves require through-thickness measurements [5], which appears to be impractical in most industrial applications. Therefore, the methods that do not require the double-sided access are of great interest [6], which motivated the research presented in this paper.

The experiments presented in this paper were aimed to investigate the possibility of designing an air-coupled NDT system for the assessment of composite structures. Two types of damages, typical for composite materials, were evaluated: delaminations and cracks. Based on these tests, the phenomena occurring during the interaction of symmetric and antisymmetric modes with the defects will be presented and discussed. Finally, an example feature extraction procedure will be used to produce C-scan images.

THEORETICAL BACKGROUND

In order to place the following work into its context, principles of leaky LWs generation and reception by the means of air-coupled transducers will be briefly outlined in this section. Next, the phenomena encountered during interaction of Lamb waves with the defects specified above will be described.

Air-coupled Lamb waves

LWs existing in thin plates are dispersive and multimodal, which means that an infinite number of symmetric and antisymmetric modes can exist for each frequency. Numerous Lamb modes that are present in received ultrasonic signals make its interpretation difficult and therefore, the use of mode-selective excitation and reception techniques is beneficial. A single mode excitation by means of air-coupled transducers can be performed based on the principles presented in **Figure 1**. In order

to excite a single (or at least an enhanced mode) the incident angle of the emitter φ_A has to be set to a value which can be calculated from the Snell's law:

$$\varphi_A = \sin^{-1}\left(\frac{c_{air}}{c_{LW}}\right) = \sin^{-1}\left(\frac{\lambda_{LW}}{\lambda_{air}}\right), \quad (1)$$

where: c_{air} denotes sound velocity in air, and c_{LW} phase velocity of the excited LW. λ_{air} and λ_{LW} denote respectively the wavelengths in air and the inspected plate. The same principle can be used to make a receiver sensitive to the selected mode (i.e. $\varphi_A = \varphi_S$).

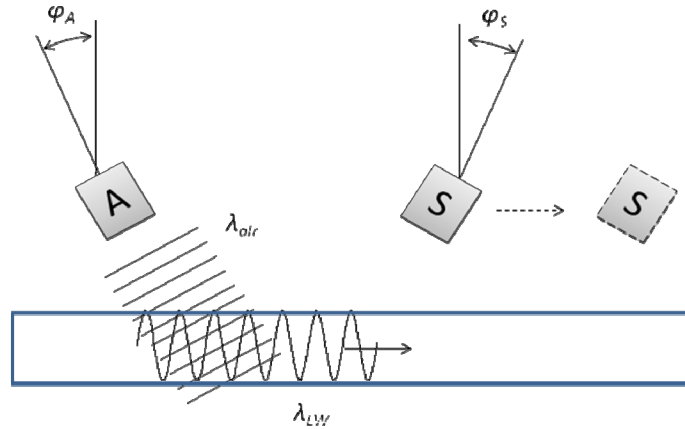


Figure 1. Principle of Lamb waves generation and reception using air-coupled transducers.

Another reason for the selective excitation/reception of LWs is that various modes are sensitive to different types of flaws [7]. Moreover, different phenomena can occur when a LW interrogates with damage. Damage detection and characterization techniques rely on the feature extraction of the captured signals that are specific for different damage types. For instance, a crack causes normally scattering, therefore the reflected wave can be an indicator used in damage detection and localization procedure. Another phenomenon that may take place at a damage interface is mode-conversion, e.g., an S_0 mode incident at a defect produces an A_0 mode. Besides the energy conversion, its dissipation caused by damage is a common phenomenon and therefore the analysis of the wave amplitude decay can be a valuable source of information.

EXPERIMENTAL SETUP

The experiments were carried out with the use of two air-coupled transducers: The emission is provided by means of a non-contact transducer NCG350-D50 with the resonant frequency of 350 kHz, provided by Ultrason Group, USA. The membrane type, non-contact wide band transducer type mBAT-1 manufactured by Micro-Acoustics, Canada was used as a receiver. The transducers were mounted in a precise mechanical scanner, presented in **Figure 2a**, which was used to shift the sensor along the wave's propagation path and enabled obtaining B-scan images for the each measured profile [8]. Moreover, the scanner gimbals facilitated adjustment of the incident angle of the transducers to excite and receive Lamb modes selectively. For instance, to obtain the enhanced A_0 mode the angle was set to 17° . To enhance the

rapid S_0 mode the incident angle was set to 4° . The incident angles could be adjusted separately, e.g. the actuator could be used to evoke the S_0 mode and the sensor could be set to capture the enhanced A_0 mode.

A broadband linear chirp signal with the frequency band from 100 to 500 kHz was used as an excitation. The received signals were then cross-correlated with the excited signal using matched filtration technique. The experiments were carried out on two 1.2 mm thick $[0^\circ \ 45^\circ \ -45^\circ \ 0^\circ]$ 4-ply CRFP with defects. The first plate had an artificial delamination, located at the position 130 mm (Fig.2.b) produced in the manufacturing process with the use of a Teflon inclusion inserted between the middle layers. The second plate was damaged using a high energy impact that produced crack.

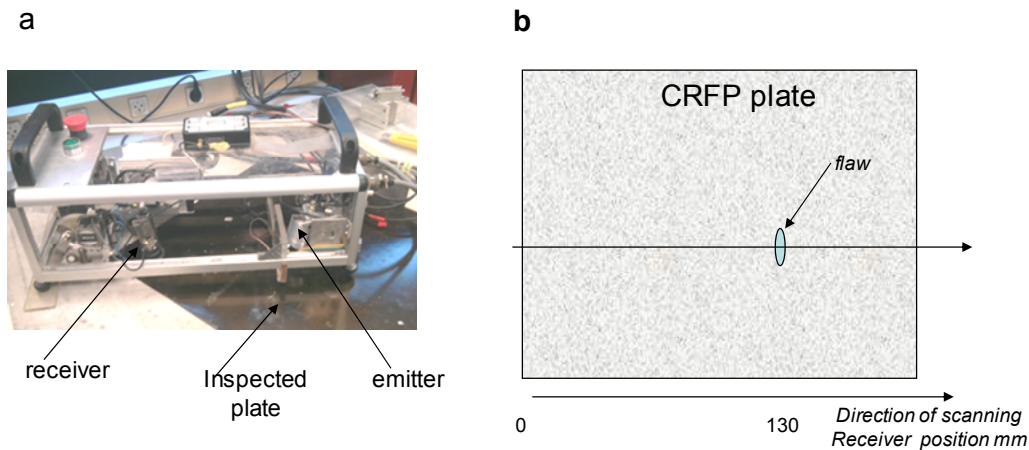


Figure 2. Mechanical scanner used in the experiments [8] a), experimental setup at the first plate b).

RESULTS

In the following section, examples of LWs interaction with defects will be illustrated using data obtained from a single scan profile presented in the form of B-scan images. Next, a C-scan image based on the extraction of the difference in signals decay for the undamaged and damaged structure will be presented.

Interaction of Lamb waves with a crack

The first experiment was conducted on the CRFP plate with crack. In order to observe the interaction of LWs with the defect the incident angles of the emitter and sensor were set to 4° . The scanning was performed along a line perpendicular to the edge of the crack with a step of 1 mm as shown in Fig.2b. The signals captured at the successive points can be seen in **Figure 3a** as a B-scan image. The defect is localized, as expected, at the position 130 mm. A clear S_0 mode incident at the defect can be seen. Moreover, the diffraction at the defect is clearly seen and a weakly pronounced reflected S_0 wave can also be observed, although the angle of the sensor was not suitable to capture the wave propagating in the direction of the reflected wave. The root-mean-squared (RMS) amplitude of the incident S_0 mode is presented in **Figure 3c**. A rapid drop of the amplitude can be seen in position 130 mm, that is after the wave has passed the crack.

The next experiment was performed to investigate the interaction of A_0 mode with the crack and therefore the incident angles of the emitter and receiver were set to 17°

(c_{LW} between 500 and 1500 m/s.). From the B-scan image, presented in **Figure 3b**, a clear incident A_0 mode can be seen. Moreover, a clear drop of the signal amplitude can be seen after the crack location. The decay of the signal amplitude is even more distinct in the amplitude plot presented in **Figure 3d**.

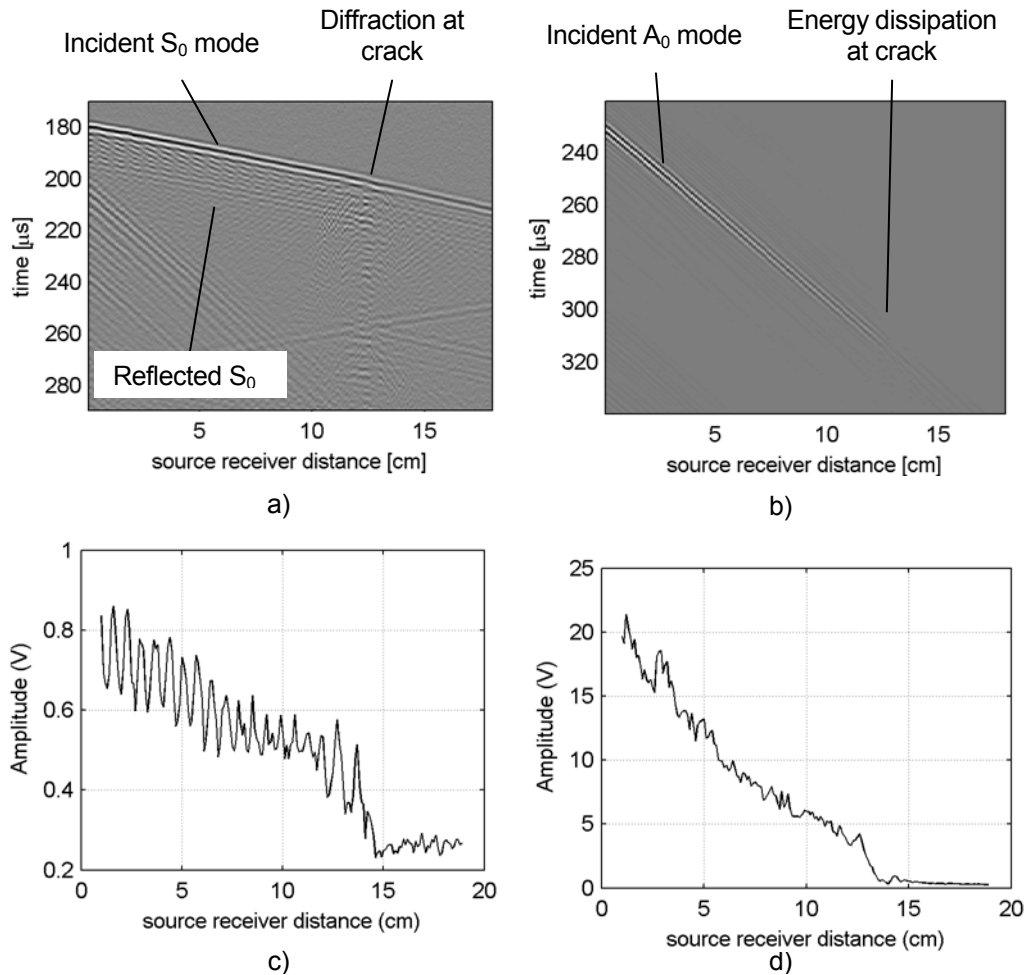


Figure 3. B-scan images illustrating the interaction of LWs with a crack in CFRP: S_0 mode a) and A_0 mode b) (note difference in time scales). RMS amplitudes of the time-gained signals for S_0 mode c), and A_0 mode d) (note difference in amplitude scales).

Comparison of the wavefront slopes corresponding to the incident S_0 and A_0 modes, in the B-scans in **Figure 3a** and **b**, respectively, shows as expected, that the S_0 mode is much faster than A_0 mode. Moreover, a smaller decay of the S_0 mode compared to A_0 mode can be observed in **Figure 3c** and **d**. Note the amplitude drop of in both cases at the crack that can be explained by the energy dissipation at the damage. Another possible reason for the amplitude reduction can be mode-conversion that results in a new mode which perhaps cannot be captured by the sensor due to its insensitivity to the velocity of the mode-converted wave.

Another experiment was performed with the aim to investigate the mode-conversion. In the previous tests it was difficult to observe this phenomenon since the incident angles of the actuator and sensor were equal and therefore both transducers were most sensitive to the same mode. In this experiment, the angle of the emitter was set to 4° and the angle of the receiver was set to 17° , in order to excite/sense the S_0/A_0 modes respectively; scanning was performed with the step of 2 mm. Results of this

experiment are presented in Fig. 4. Notice that although the emitter was set to excite the pure S_0 mode, this mode is hardly visible in the **Figure 4a**, because the sensor is insensitive to the S_0 mode. Moreover, an undesired incident A_0 mode can be observed in the B-scan, which means that in fact the transmitter did not excite the desired pure mode but also the second mode. From the result shown in Figure 4a it can be seen as lines originating in the vicinity of the source-receiver distance of 130 mm, with the same inclination as the incident A_0 mode. In the next step the RMS of the signals corresponding to the incident S_0 mode was calculated and presented in Figure 4b. It can be observed that the damage induces a significant signal increase. This surprising phenomenon might be interpreted as an interference of the incident S_0 and converted A_0 modes.

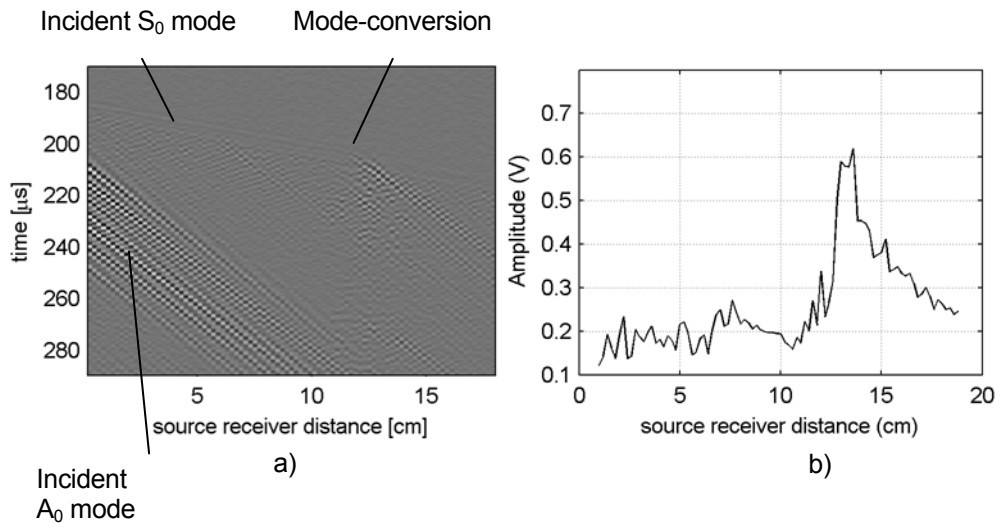


Figure 4. Mode conversion in the CFRP with crack a). Amplitude distribution of the signals from the B-scan c).

Interaction of Lamb waves with delamination

Previous sub-section dealt with the interaction of two Lamb modes with the crack. Results of similar experiments conducted for the panel with delamination are presented below. Two scans with the enhanced S_0 and A_0 modes were acquired with the scanner step of 2 mm and the results can be seen in **Figure 5**. In the first B-scan, presented in **Figure 5a**, the perturbation of the signal due to the delamination can be observed. An analysis of the signals' amplitude, presented in **Figure 5c**, shows that a rapid change in its attenuation can be seen in the damaged area, similar local increase of the A_0 mode attenuation caused by the delamination can also be observed in **Figure 5b** and d.

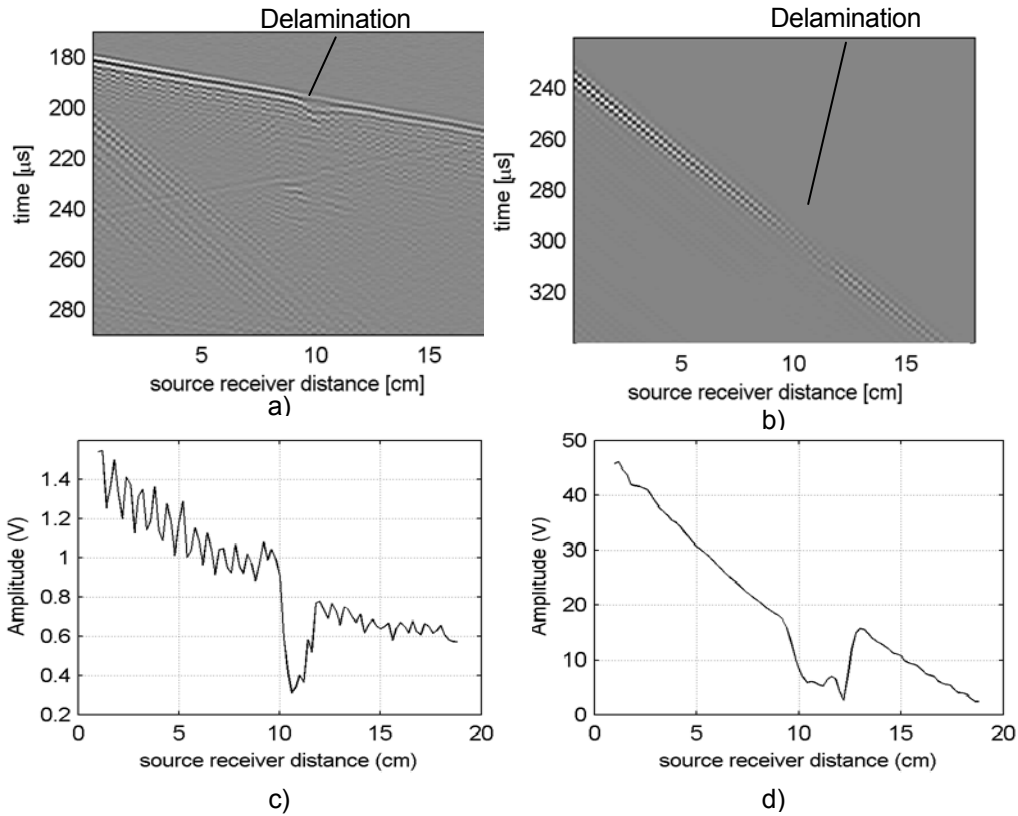


Figure 5. Interaction of LWs with delamination in CFRP. B-scan images obtained using a selective generation and sensing of a) S_0 and b) A_0 mode. Distribution of the signal amplitude from the B-scan S_0 and A_0 , respectively c) and d).

C-scan images based on attenuation analysis.

As it was shown in the previous sections various features of the signals can be used for damage detection. An example of attenuation analysis used to create a C-scan image will be presented below. In the experiment the transducers were set to excite/receive A_0 mode and a set of 50 parallel B-scans spaced with 5 mm were acquired over the CFRP plate along the x -axis direction, for y varying from 0 to 25 mm. The delamination was located in the area $12 < x < 15$ mm and $12 < y < 15$ mm indicated at Fig. 6b.

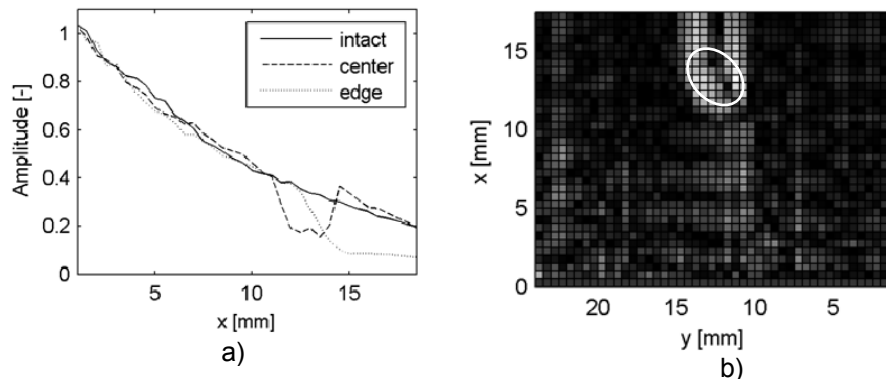


Figure 6. Instantaneous amplitude of the signals obtained for the inspected surface a). C-scan obtained for the CFRP with delamination b).

The ultrasonic signals were acquired in the both delaminated and intact area of the CFRP and then the RMS of the incident wave amplitude was calculated. Examples of amplitude distribution obtained for profiles captured in the intact area and in the center and on the edge of delamination are presented in Fig. 6a. The damaged and undamaged attenuation profiles can be easily distinguished. The profiles captured for the intact plate area were averaged to calculate a reference attenuation profile. Next an absolute value between the reference profile and the measurements were calculated and displayed as a C-scan image in Fig. 6b. The brighter area of the image clearly indicates the delamination region. Note that although the wave passes through the damage, it is not attenuated completely for all propagation paths. It appears that the wave is attenuated more when it propagates along the edge of the delamination than when it passes through its center.

CONCLUSIONS

We have shown that both A_0 and S_0 Lamb wave modes can be selectively excited and received using air-coupled transducers in the pitch-catch configuration. The A_0 mode due to its higher out-of-plane displacement presents normally higher amplitudes compared to the S_0 mode, which however, has a lower attenuation coefficient.

Various phenomena that occur during the interaction of a LW with a defect, such as, mode conversion, mode reflection, diffraction and signal attenuation can be indirectly observed in the received signals. Thus, extracting the signal features characteristic specific for the above phenomena facilitates detecting and locating the damage. We have shown an example how the C-scan built up of instantaneous amplitude profiles can be used for effective damage detection and localization.

REFERENCES

- [1] W. Grandia and C. Fortunko, "NDE applications of air-coupled ultrasonic transducers," in *Ultrasonics Symposium, 1995. Proceedings., 1995 IEEE*, vol. 1, pp. 697–709 vol.1, nov 1995.
- [2] J. Salazar, A. Turo, J. Chavez, J. Ortega, and M. Garcia, "High-power high-resolution pulser for air-coupled ultrasonic NDE applications," *Instrumentation and Measurement, IEEE Transactions on*, vol. 52 (6), pp. 1792–1798, 2003.
- [3] S. Kelly, G. Hayward, and T. Alvarez-Arenas, "Characterization and assessment of an integrated matching layer for air-coupled ultrasonic applications," *Ultrasonics, Ferroelectrics and Frequency Control, IEEE Transactions on*, vol. 51, pp. 1314–1323, oct. 2004.
- [4] D. Schindel, D. Hutchins, and W. Grandia, "Capacitive and piezoelectric air-coupled transducers for resonant ultrasonic inspection," *Ultrasonics*, vol. 34, no. 6, pp. 621–627, 1996.
- [5] D. Schindel and D. Hutchins, "Through-thickness characterization of solids by wideband air-coupled ultrasound," *Ultrasonics*, vol. 33, no. 1, pp. 11–17, 1995.
- [6] M. Castaings, P. Cawley, R. Farlow, and G. Hayward, "Single sided inspection of composite materials using air coupled ultrasound," *Journal of Nondestructive Evaluation*, vol. 17, pp. 37–45, 1998. 10.1023/A:1022632513303.
- [7] B. C. Lee and W. J. Staszewski, "Lamb wave interaction with structural defects: modeling and simulations," vol. 5049, pp. 146–155, SPIE, 2003.
- [8] B. Piwakowski, P. Safianowski and M. Kaczmarek, Automated NDT by Non-contact Surface Waves, presented at the Int. Congres of Ultrasonics, ICU2011, Gdansk, Poland, Sept. 2011